

Final Report

MONITORING THE SPATIALLY AND TEMPORALLY COMPLEX ACTIVE DEFORMATION FIELD IN THE SOUTHERN BAY AREA

Grant 01-HQGR-0196

Roland Bürgmann, University of California, Berkeley

Department of Earth and Planetary Science

307 McCone Hall

Berkeley, CA 94720-4767

Telephone: (510) 643-9545; FAX (510) 643-9980; burgmann@seismo.berkeley.edu

URL: <http://www.seismo.berkeley.edu/~burgmann>

NEHRP Program Element: I, Products for Earthquake Loss Reduction

Keywords: Surface Deformation, Geodesy, GPS-Campaign

We use the Global Positioning System (GPS), Synthetic Aperture Radar Interferometry (InSAR), and repeating identical micro-earthquakes to gather information on crustal deformation and earthquake hazard in the southern San Francisco Bay region. The research is composed of collection and analysis of space geodetic data, analysis of micro-earthquakes for fault-slip information, and modeling and interpretation of those results in the context of fault slip rates, the locked or aseismically creeping nature of individual segments of the southern Bay area fault system, and earthquake potential from those faults. Most of the transient deformation associated with the 1989 Loma Prieta earthquake apparently ceased by about 1994. However, transient deformation anomalies such as slow earthquakes persist on the San Andreas Fault in the region of transition from locked to creeping behavior and likely influence the stress and thus earthquake potential in the region.

Research supported by the U.S. Geological Survey (USGS), Department of the Interior, under USGS award number 01HQGR0196. The views and conclusions contained in this document are those of the authors and should not be interpreted as necessarily representing the official policies, either expressed or implied, of the U.S. Government.

1. Introduction

The southern Bay Area is a structurally complex region of the North American-Pacific plate boundary. North of the creeping section of the San Andreas Fault (SAF) near the town of San Juan Bautista (SJB), the Calaveras Fault (CF) diverges from the SAF and fault slip from the creeping section is partitioned between the two. Plate motion is also accommodated on the active Sargent and Quien Sabe faults. After the SAF/CF junction, both faults transition from creeping to fully locked. North of the transition zone, the SAF last slipped in the 1906 earthquake and represents a significant seismic hazard. This region also contains the epicentral region of the 1989 Loma Prieta (LP) earthquake which occurred in the Santa Cruz Mountains on a secondary fault close to the SAF. The LP earthquake accelerated deformation rates throughout the southern Bay Area for 5-6 years, including regional deformation from exponentially decaying afterslip, increased compression within the Foothills thrust belt (Bürgmann, 1997b) and increased slip on the Pajaro section of the SAF, just north of SJB (Wilber and Bürgmann, 1999). The effects of the Loma Prieta earthquake are still felt on the Calaveras fault, where surface creep has yet to return to its pre-LP rate. Time dependent deformation also occurs in the form of creep events and slow earthquakes; primarily located in the transition zone of the SAF. Geodetic measurements of strain redistribution due to these events could shed light on the processes controlling the occurrence of earthquakes in this region.

We yearly occupy our Global Positioning System (GPS) network in the southern Bay area, spanning the epicentral region of the Loma Prieta earthquake, the Calaveras fault and its juncture with the San Andreas fault. The GPS data are integrated with other data sets such as the creepmeter records on the Hayward, Calaveras and San Andreas faults (Data collected by USGS, and CU Boulder) and borehole strain data from instruments installed near San Juan Bautista (CSIRO and USGS). Differential interferometric synthetic aperture radar (InSAR) has been effectively integrated with GPS data to perform a joint inversion for slip on the Hayward fault (Bürgmann et al., 2000). However its use over regions that are sparsely urbanized and contain dense vegetation, such as the SAF near SJB, is limited by decorrelation noise. We are implementing a method, similar to the “Permanent Scatterer” method of Ferretti et al. (2001), to identify stable pixels based on their amplitude and thereby construct a sparse grid of point capable of detecting local deformation. We are also pursuing subsurface slip rates on creeping members of the SAF system using repeating micro-earthquakes. Observations of recurrence intervals of identical micro-earthquakes to infer variations in slip rate on the fault surface (Nadeau and McEvilly, 1999). Bürgmann et al. (2000) applied this technique to the northern

Hayward fault and found evidence for aseismic slip throughout all depths of the segment, further substantiating the results of a formal inversion of GPS and InSAR data. Current data show evidence for a repeating slip transient with a period of three years on the northern part of the creeping SAF.

The primary objective of this project is to monitor the spatially and temporally complex active deformation field in the southern Bay Area. This report will focus on three aspects of this investigation:

- Update of GPS measured crustal deformation.
- The use of InSAR to detect and characterize transient slip events in the transition zone of the SAF.
- The use of repeating micro-earthquake data to determine steady and transient subsurface slip rates on aseismically slipping fault segments.

2. Results

In recent years we have increased our network of 23 sites, occupied yearly, in the Southern Bay Area to include more stations in the SJB/Hollister area. We are now in a position to better characterize the transition of the SAF from locked to creeping and to better observe variations in the distribution of slip between the Sargent, San Andreas and Calaveras faults. Figure 1 shows interseismic velocities of stations in the SJB/Hollister area determined from yearly measurements from 1991-2001. Figure 1 uses campaign mode data from the University of California, Berkeley and the USGS as well as data from continuously operating BARD sites. Data collected by UC Berkeley is processed with Bernese GPS processing software from the University of Bern.

An interesting feature of the data is the continued motion on the Calaveras fault despite the absence of surface creep since the Loma Prieta earthquake (Manaker et al., 2001, submitted to JGR). Better data coverage will reveal any changes in fault slip at depth following LP. The locked to creeping transition is visible as an increase to the southeast in the velocity contrast across the SAF. Although stations are too sparsely located to characterize this transition at depth, these velocities can provide a framework for more detailed InSAR measurements.

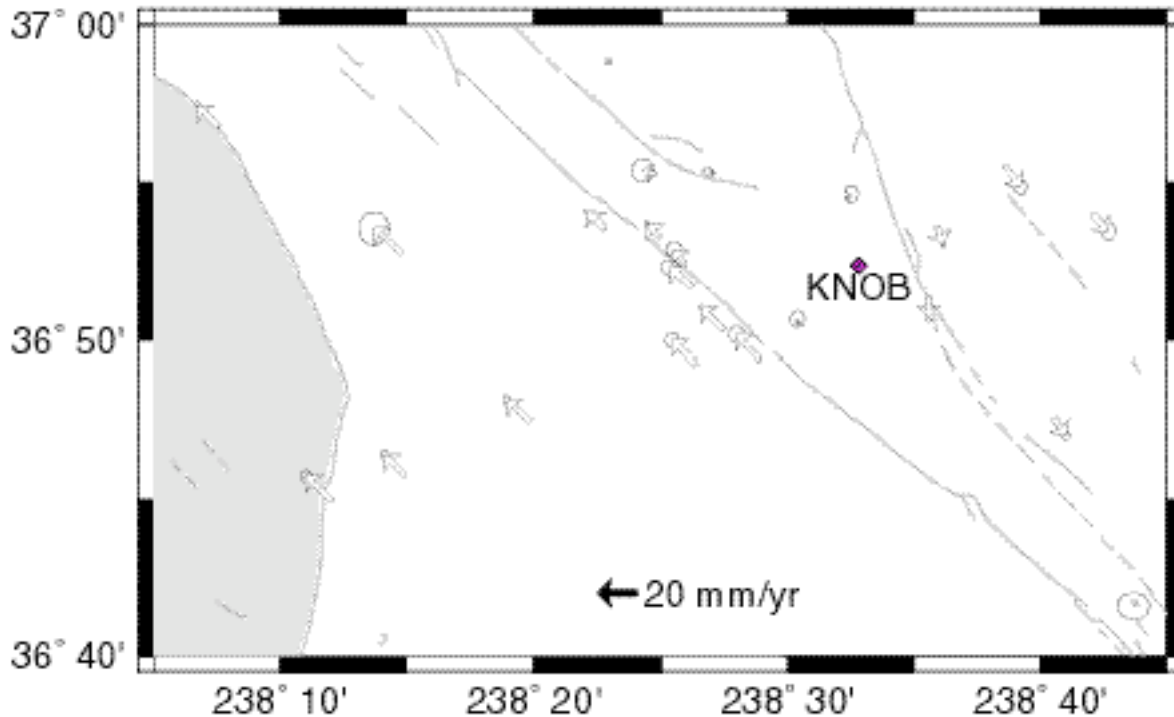


Figure 1. Compilation of continuous and campaign GPS derived velocity field in the SAF-Calaveras juncture area. Data are from our own and USGS measurements. The displacement field is shown relative to station KNOB outside the town of Hollister.

Transient fault slip on Bay area faults from InSAR measurements Geodetic measurements of surface displacements surrounding a fault can be used to determine subsurface slip rates on dislocations in an elastic half-space model. If fault slip occurs at relatively shallow depth, as is commonly the case during slip transients on creeping faults, such measurements have to be closely spaced around the slip patch to adequately determine basic parameters such as rupture area and depth. Precisely surveyed GPS sites in the San Francisco Bay area are generally spaced more than 10 km apart and it is therefore difficult to detect the deformation field of a shallow event from existing point measurements alone. Borehole strainmeters and creepmeters, which have been the primary instruments to record slip transients in this region, also suffer from sparse spatial distribution. Space based Interferometric Synthetic Aperture Radar (InSAR) can map ground deformation at 10s-of-meter spatial resolution with sub-cm precision. The improved spatial resolution makes InSAR an excellent tool for observing shallow fault movement with small deformation rates such as along strike creep rate variations as the SAF transitions from locked to fully creeping and slow earthquakes and other transients.

Surface displacement is computed from the interferograms by converting the phase delay between scenes into line-of-sight range change rates. Surface displacements and resulting range

change are related as $\Delta\rho = \Delta\vec{d} \cdot \vec{e}$, where $\Delta\rho$ and $\Delta\vec{d}$ are the range change and surface displacement vectors, respectively, and \vec{e} is the unit vector in the range direction (Bürgmann et al., 2000). We process interferograms using the Repeat-Orbit Interferometry Package (ROI-PAC) developed at the Jet Propulsion Laboratory.

With its good spatial resolution and high precision, InSAR is capable of detecting small areas and small amounts of deformation. However, the method is dependent on stable surface properties to maintain good correlation between scenes used to form the interferogram. The signal detected by the SAR satellite is an average of the backscattered energy from all the reflectors in the satellite footprint. If the arrangement of scatterers changes, decorrelation occurs and the phase difference between the two scenes will reflect that reorganization of objects and not surface deformation. Urban areas, bedrock and arid regions provide very good correlation; they can be stable for several years. Areas with a densely vegetated surface, like much of the Southern Bay Area, can destabilize within a month. Decorrelation also becomes a problem when the satellite orbit is sufficiently dissimilar in both scenes. When the orbits have large perpendicular baselines, the satellite will view the scattering objects as having a different arrangement and the two measurements will not be comparable. This prevents certain scenes from being combined with each other to form an interferogram and severely limits the time spans that can be covered.

Traditionally interferometry has relied on capturing the deformation pattern within an area of good correlation. The phase information can then be correctly unwrapped to determine deformation rates. Isolated patches of correlated phase must be connected to each other using an independent source, such as GPS, to estimate the number of intervening phase cycles. When these isolated patches are as small as a single pixel, they are completely obscured by the surrounding regions of decorrelation noise. The Permanent Scatterer Method, as proposed by Ferretti et al. (2001), identifies these stable pixels by looking for points with stable amplitudes (both bright and dim) and phase measurements that are coherent through time. Points selected by the Permanent Scatterer Method are often buildings whose corner reflecting walls reflect much more brightly than any surrounding vegetation. With this observation, we identify stable scatterers simply as points with consistently high amplitudes that are distinct from their surroundings. Corner reflectors also appear identical to the satellite regardless of reasonable variations in its orbit. This allows interferometric pairs with a large perpendicular baseline to be used that otherwise have prohibitive levels of decorrelation noise. The result is a network of point measurements equivalent to a very dense GPS array.

Figure 2A is the average amplitude of seven synthetic aperture radar (SAR) scenes collected

by the European Space Agency's ERS 1 & 2 spacecrafts from 1993 – 1998. The region shown is a sub-section of descending track 299, frame 2861 containing the town of San Juan Bautista.

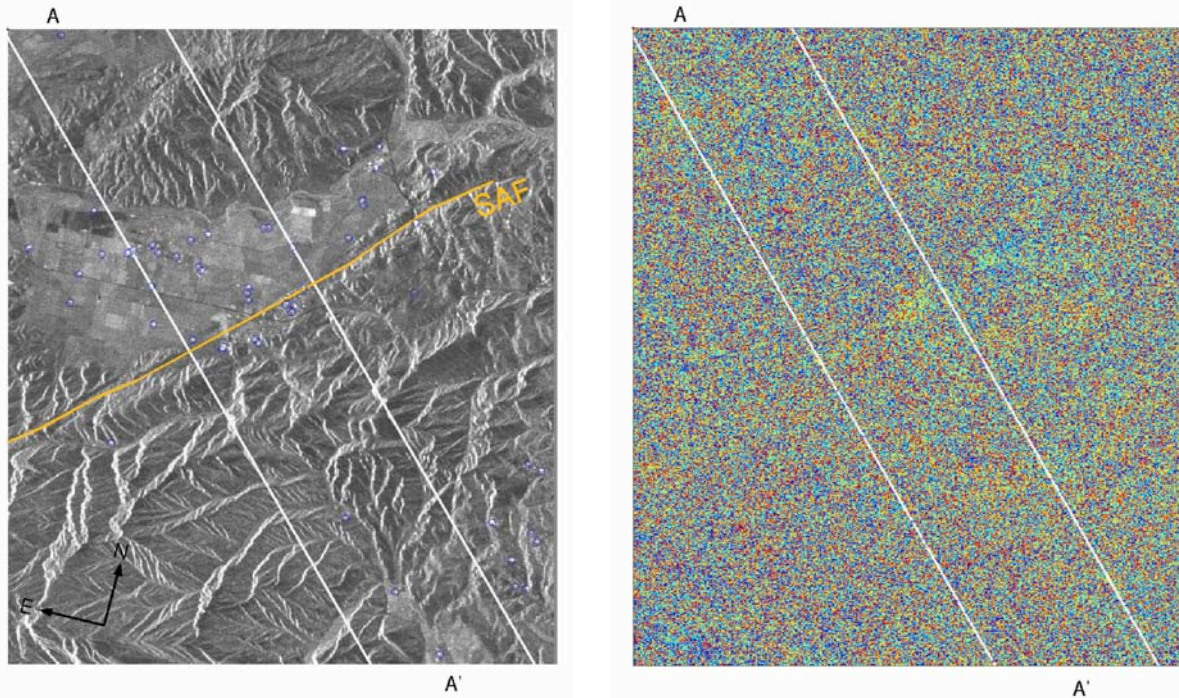


Figure 2A Average of seven SAR amplitude images from 1993-1998. Red circles are proposed stable scatterers; blue line is the trace of the SAF. Image is in Range/Azimuth coordinates; note patchwork fields in San Juan Valley for scale.

Figure 2B Unfiltered interferogram from May 19, 1996 to August 18, 1997 corresponding to the area shown in figure 2A. In both figures, white lines delineate the width of profile AA' shown in figure 2C.

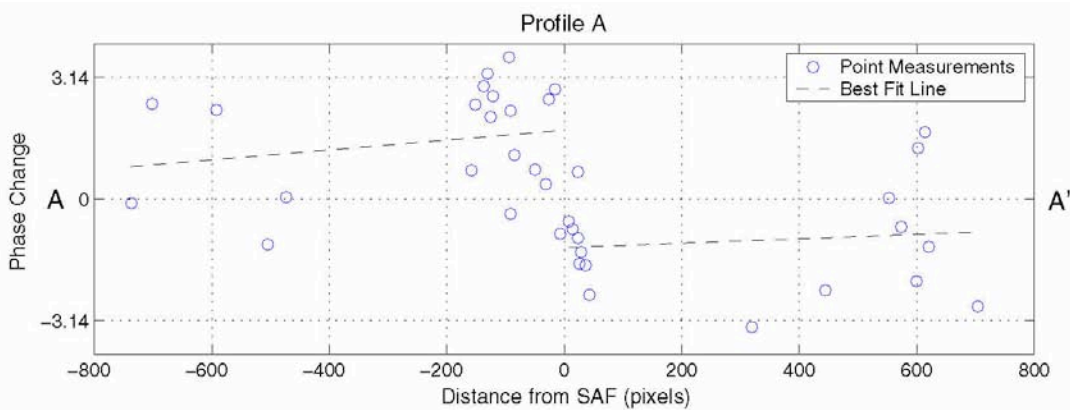


Figure 2C Profile of proposed stable scatterers shown as red circles in figure 2A. SAF is located at pixel 0. Dashed lines are least squares fits to each half of the data.

Stacking preserves stable high amplitudes and reduces random noise. Points with high amplitudes in the midst of low amplitude points were chosen as proposed stable scatterers (red

circles). Most points have an average amplitude greater than three standard deviations above the mean of the whole image. Air photos to the south of the region shown confirm that the majority of identified points are buildings. Figure 2B shows an interferogram (from May 19, 1996 and August 18, 1997) dominated by decorrelation noise. Profile AA' in Figure 1C is a plot of the proposed stable scatterers (red circles in figure 2A) between the white lines extracted from the interferogram shown in figure 2B. The dashed lines are fit by least squares to the point measurements on either side of the SAF (located at pixel 0); where they are offset from each other by 3 radians. A phase delay of 3 radians corresponds to either 4-5 cm of right lateral slip on the SAF, or 1.5 cm of uplift of the SJB valley in the 16 months spanned by this pair. Creepmeter XSJ2 recorded one creep event for a total of 5 mm of surface creep during the same time period. Sylvester et al. (1995) observed highly variable rates (0.5-3cm/yr) of vertical motion, usually valley subsidence across the SAF in SJB, possibly due to ground water removal in the valley. It is thus expected that the measured range change will contain some vertical motion. We are working on incorporating ascending track frames into this analysis to separate vertical and horizontal motions.

Regional deformation in the southern Bay Area from InSAR measurements

Fault motions in the southern Bay Area include significant amounts of surface creep and shallow transient slip. This requires geodetic measurements to be closely spaced around the slip patch in order to adequately determine basic parameters such as slip surface area and depth. Even with the expansion and densification of our campaign GPS network in the past several years, stations are generally spaced more than 10 km apart, making it difficult to detect the deformation field of a shallow event from point measurements alone. Space-based Interferometric Synthetic Aperture Radar (InSAR) can map ground deformation at 10s-of-meter spatial resolution with sub-cm precision. The improved spatial resolution makes InSAR an excellent tool for observing shallow fault movement with small deformation rates such as along-strike creep rate variations as the SAF transitions from locked to fully creeping and the 1992, 1996 and 1998 sequence of slow earthquakes on the SAF near San Juan Bautista (SJB).

Surface displacement is computed from the interferograms by converting the phase delay between scenes into line-of-sight range change rates. Surface displacements and resulting range change are related as $\Delta\rho = \Delta\vec{d} \cdot \vec{e}$, where $\Delta\rho$ and $\Delta\vec{d}$ are the range change and surface displacement vectors, respectively, and \vec{e} is the unit vector in the range direction (Bürgmann et al., 2000). We process interferograms using the Repeat-Orbit Interferometry Package (ROI-Pac) developed at the Jet Propulsion Laboratory and the Statistical-cost Network-flow Algorithm for

Phase Unwrapping (SNAPhU) developed at Stanford University (Chen and Zebker, 2001).

With its good spatial resolution and high precision, InSAR is capable of detecting small areas and small amounts of deformation. However, areas with vegetated ground cover, like most of the southern Bay Area, are very susceptible to decorrelation noise. The interferograms covering this area often contain only small isolated patches of coherent signal. Our data processing strategy is therefore driven by the goal of maximizing the spatial coverage of each interferogram. We have begun this year to include SNAPhU in our processing routine; this algorithm preserves small patches of coherent phase and provides a rigorous estimation of the phase cycle offset between them.

Atmospheric delays are also a major error source for InSAR. Atmospheric errors are considered random in time and can therefore be minimized through data stacking. In an attempt to again maximize the spatial coverage of useful data, we have implemented a novel approach to data stacking. We allow the data sources (input interferograms) to vary from pixel to pixel, including only those sources with coherent data at that point and only those points with data from three or more sources. Each pixel is then weighted according to the time spanned by its inputs. Figure 3 shows the result of stacking nine input interferograms using data from the European Space Agency's ERS 1 & 2 spacecrafts from 1995-2000 (Track 299 Frame 2861). Figure 3b actually contains greater spatial coverage than any of its individual input interferograms. Figure 3c illustrates the number of images with coherent data available at each point.

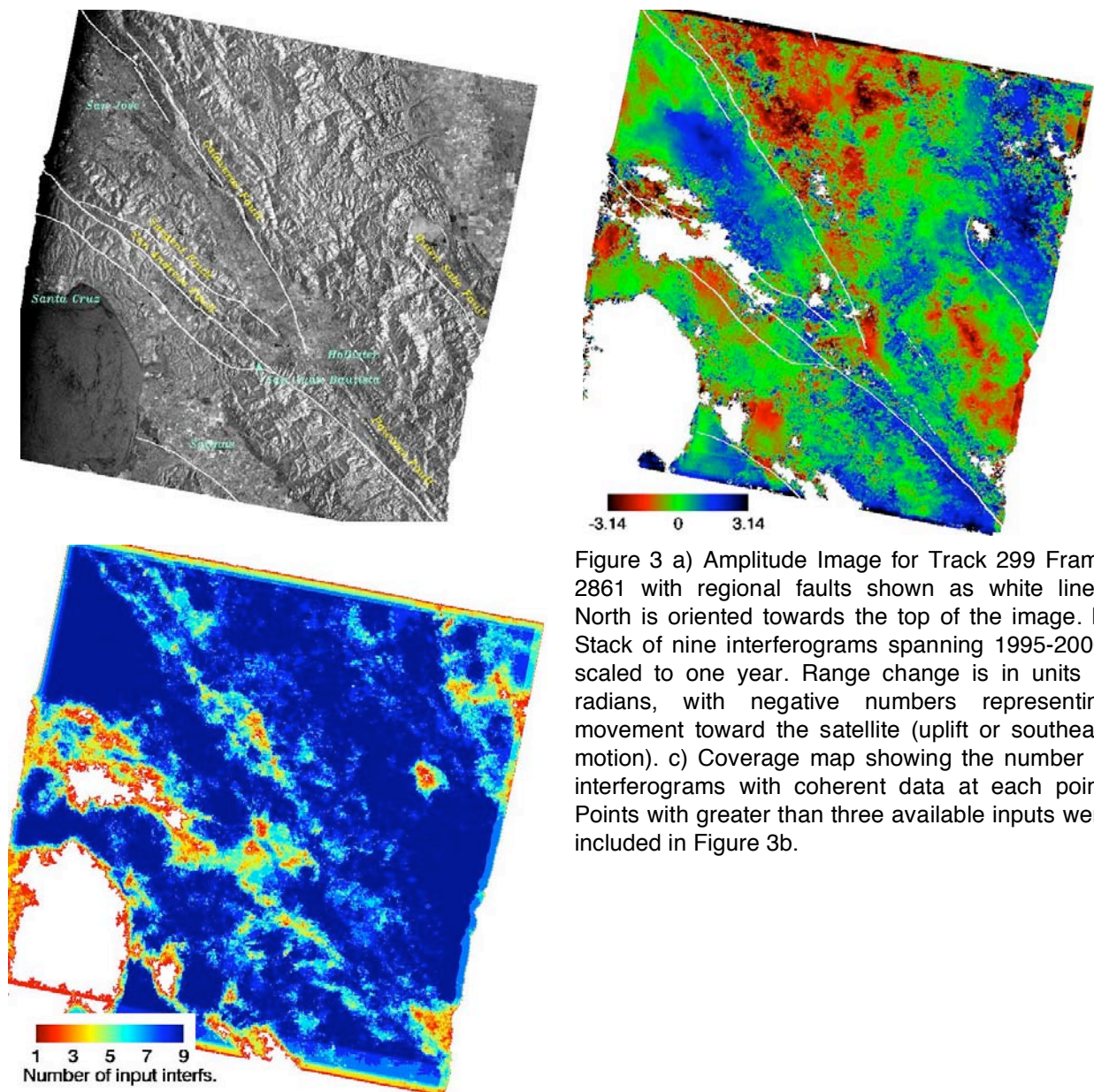


Figure 3 a) Amplitude Image for Track 299 Frame 2861 with regional faults shown as white lines. North is oriented towards the top of the image. b) Stack of nine interferograms spanning 1995-2000, scaled to one year. Range change is in units of radians, with negative numbers representing movement toward the satellite (uplift or southeast motion). c) Coverage map showing the number of interferograms with coherent data at each point. Points with greater than three available inputs were included in Figure 3b.

Time dependent creep of the SAF near San Juan Bautista from repeating micro-earthquakes.

The juncture between the San Andreas fault and the southern Calaveras fault is a highly complex area where subsurface seismicity does not always follow surface fault traces and where secondary sub-parallel faults, such as the Quien Sabe fault zone, may play an active role in accommodating local shear deformation. The goal of this part of the investigation is to determine the slip rate distribution of these faults at the SAF/CF juncture using characteristic microearthquake-defined subsurface slip rates and surface geodetic measurements. To date, we

have determined initial subsurface slip rates using the previously derived empirical formula of Nadeau and McEvilly (1999) which combine recurrence intervals and moment magnitudes of repeating earthquakes to determine slip rates at depth for each individual repeating earthquake sequences. Initial sequence estimates of slip rates for the San Andreas, southern Calaveras and Quien Sabe fault zone are found to be between 12 and 24 mm/yr, 4 and 13 mm/yr, and 4 and 10 mm/yr, respectively. Due to the low rate of secular slip, the magnitude threshold of the NCSN catalog, and the limited observation time (17 years), we have only identified pairs of repeating earthquakes on the southern Calaveras fault and Quien Sabe fault zone. These limitations also make the estimates on these faults particularly uncertain. Nevertheless, the simple fact that we find repeating earthquakes on these faults is important because it indicates that they are slipping at depth even though there may be no surface expression of this slip. For example, relatively high subsurface slip rates were found on the Quien Sabe fault zone (4 to 10 mm/yr.) relative to surface slip rate estimates there of only 1 ± 1 mm/yr (Bryant, 1985).

On the San Andreas fault, which has a higher rate of secular slip, we are able to see earthquakes that have recurrence intervals of about 1.8 years on average, and as little as 0.2 years in regions of rapid afterslip from large events (Nadeau and McEvilly, 2000). Figure 4 shows estimates of fault slip rates at depth and through time along a 50 km stretch of the San Andreas Fault some 20 km SE of the terminus of the 1989 Loma Prieta (LP) rupture zone.

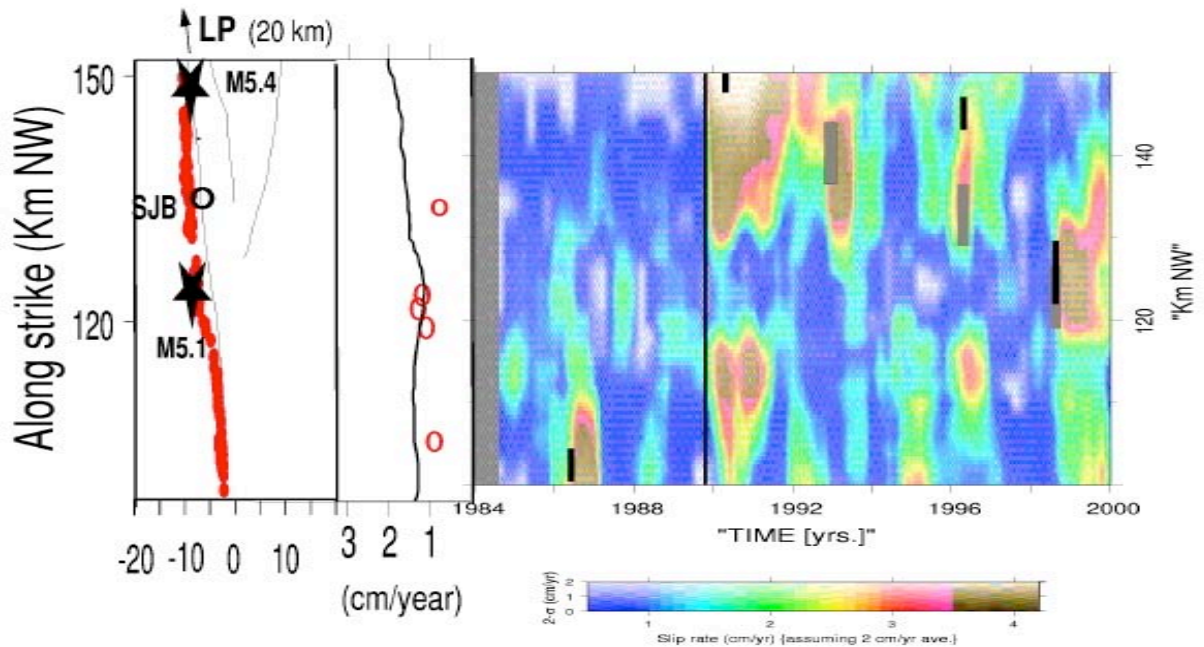


Figure 4 Slip rates are inferred from characteristic microearthquake sequences shown as red circles along the SAF trace in the left panel. The slip rates along strike averaged over the observation period 1984-2000 are shown in the curve in the middle panel. Also in the middle panel are open red circles indicating creep meter slip rates for a comparable period of time. Right Panel shows the slip rate variations for the fault through time. Also shown as short black segments are the approximate time and dimension of $> M4.5$ earthquakes on the SAF during this period. Gray segments show the locations and occurrence times of slow silent earthquakes in the area and the long black line occurring in Oct. of 1989 represents the occurrence time of the LP quake.

It is worth noting that slip rates increased dramatically in this area after LP--even at distances of up to 50 km from the rupture terminus. The increase dies down with time, but not in an exponential fashion which might be expected from afterslip. Rather pulsing with a period of about 3 years appears superposed on a generally decaying slip signature. Quiescence before and rapid afterslip also appear to be a characteristic of the smaller and slow earthquakes, though not all accelerated slip episodes are associated with moderate sized events. Slip from the characteristic quakes reflects fault deformation at depths of up to 10-15 km and is a more direct observation of tectonic slip on the fault than are surface creep and other surface based measurements. In the future we plan to integrate these earthquake slip data with data from surface and space based observations to invert for fault slip at depth with as much of the available data as possible.

The 1998 Mw 5.3 Slow Earthquake

With the increase in continuous GPS sites, slow earthquakes (SEs) have been observed on faults all over the world, especially deep in subduction zones. To date, the SAF near San Juan Bautista is the only location where slow earthquakes have occurred on an accessible strike-slip fault. The slip in these events was much closer to the surface than in subduction zone events, making this a unique and potentially very effective location to study the mechanics of slow slip. Creep- and strain-meters have been the primary instruments to record SEs in this area (Linde et al., 1996). Gwyther et al. (2000) report on the location, geometry and magnitude of one such event in August of 1998 as determined from these sparsely located instruments. We hope to better constrain the slip parameters by combining the high spatial resolution of InSAR with direct measurements of subsurface slip rates from repeating earthquake sequences.

Figure 5 shows two interferograms spanning the 1998 slow earthquake. Each exhibits a linear phase gradient aligned with the fault trace. If the signal is attributed to purely strike-slip motion, the interferograms both indicate right-lateral slip of about the same amount as recorded by creepmeters (Johanson and Bürgmann, 2002). It is expected, however, that the measured range change will contain some vertical motion. We are working on incorporating ascending track frames into this analysis to separate vertical and horizontal motions. In Figure 5b and 5c, the across-fault phase change continues to the south, possibly indicating a larger slip patch than was determined with creep- and strain- meters.

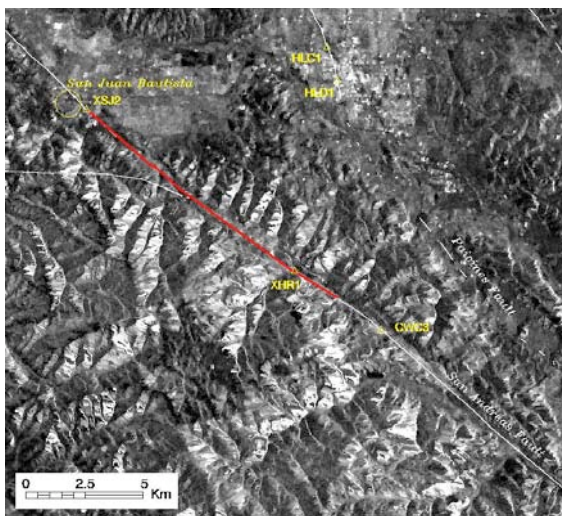


Figure 5a

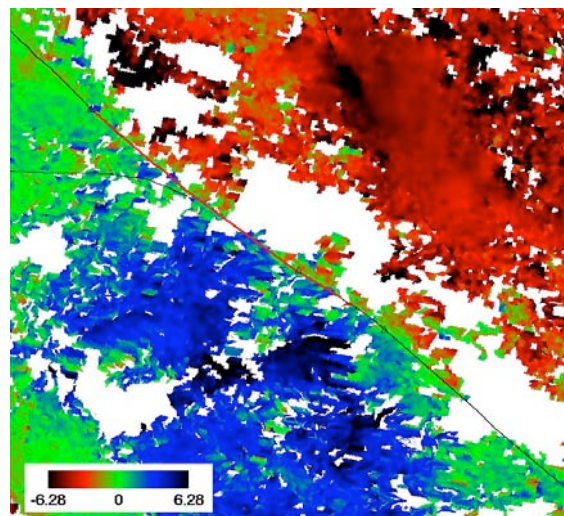


Figure 5b Aug. 18, 1997 – Oct. 12, 1998

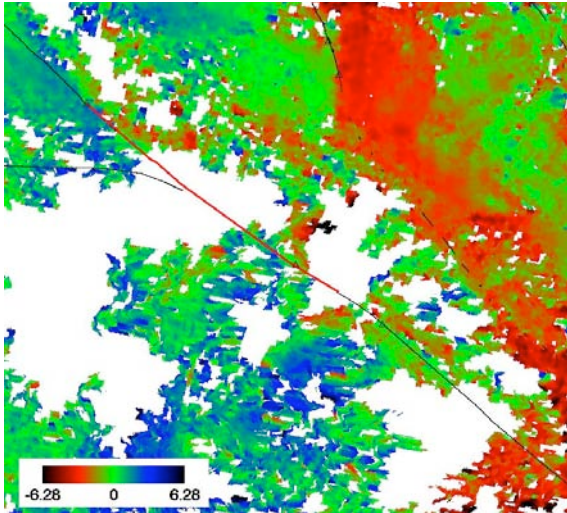


Figure 5 a) Amplitude image – subsection of Track 299 Frame 2861. Major faultlines are shown in white, red line is the length of fault rupture in the 1998 SEQ as reported by Gwyther et al. (2000) from creep- and strain-meter records. Triangles are the locations of creepmeters in the area. b) Interferogram spanning 1.15 years with a perpendicular baseline of 69 m. Range change is in units of radians, with negative numbers representing movement toward the satellite. Black lines are regional faults and red lines are same as Figure 5a. c) Same format as Figure 5b. Interferogram spans 0.96 years and has a \perp baseline of 109 m.

Figure 5c June 29, 1998 – June 14, 1999

We also attempt to use sub-surface slip rates determined from repeating micro-earthquakes to better define the rupture plane. Slip from the characteristic quakes reflects fault deformation at depths of up to 10-15 km and is a more direct observation of tectonic slip on the fault than are surface creep and other surface based measurements. In Figure 6, the color of each point indicates the amount of slip required to produce the observed clock advance (or delay) of a repeating micro-earthquake, assuming a time-predictable model.

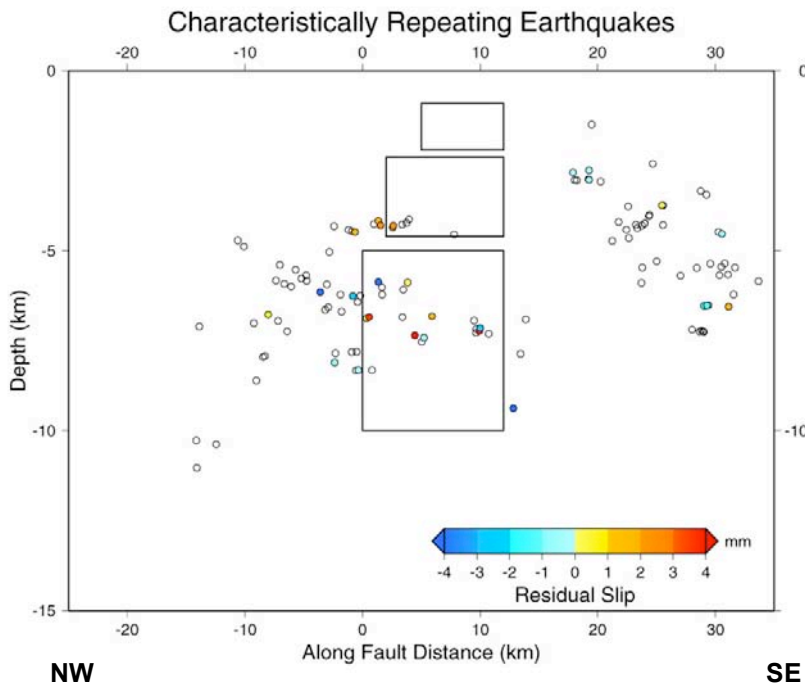


Figure 6: Circles are locations of repeating earthquake sequences on the SAF. Open circles have no data after 1998. Colored circles represent the slip surrounding the repeating earthquake rupture patch required to produce the observed clock advance or delay (negative slip) in the first occurrence of a repeating earthquake after the 1998 SEQ. All slip contributing to the clock change is attributed to the 1998 SEQ. Shown in black are the outlines of slip patches for the 1998 SEQ obtained by Gwyther et al. (2000) from creep- and strain-meter records.

The occurrence of a slow earthquake could affect characteristic earthquake sequences in two ways. First of all, if the slip patch of a characteristic earthquake in the slow earthquake rupture zone does not slip during the SEQ, then the repeating earthquake will experience a clock advance proportional to the SEQ's slip. However, if the slip patch of a characteristic earthquake experiences slip during the SEQ, then we can consider its "clock" to be reset and the next earthquake in the repeating earthquake sequence will be delayed. We would therefore expect extreme values (of either sign) of residual slip in the slow earthquake rupture area. In Figure 4, extremes of both negative and positive values occur in the rupture area of Gwyther et al. (2000) for the 1998 SEQ. By contrast, only small residuals were found for events to the southeast, well outside the SEQ rupture area. The lack of repeating earthquake below 8 km in this area does not allow us to put a depth constraint on rupture. However, the occurrence of significant residual slip to the northwest may indicate that the rupture extending further in that direction than is shown.

3. Non-technical Summary

We use the Global Positioning System (GPS), Synthetic Aperture Radar Interferometry (InSAR), and repeating identical micro-earthquakes to gather information on crustal deformation and earthquake hazard in the southern San Francisco Bay region. Most of the transient deformation associated with the 1989 Loma Prieta earthquake apparently ceased by about 1994, however, transient deformation anomalies such as creep events and slow earthquakes persist on the San Andreas Fault in the region of transition from locked to creeping. Observations of repeating micro-earthquakes show evidence for a regularly occurring slip increase at depth with a repeat time of 3-5 years. A new technique for using InSAR data is being explored to find evidence for surface deformation associated with slow earthquakes along the San Andreas fault.

4. Reports Published

- Bürgmann, R., 1997, Active detachment faulting in the San Francisco Bay area?, *Geology*, v.25, p.1135-1138.
- Bürgmann, R., Segall, P., Lisowski, M., and Svarc, J.L., 1997a, Strain development subsequent to the 1989 Loma Prieta earthquake, *U.S.G.S. Professional Paper 1550D*, p.209-244.
- Bürgmann, R., Segall, P., Lisowski, M., and Svarc, J.L., 1997b, Postseismic Strain Following the 1989 Loma Prieta Earthquake From GPS and Leveling Measurements, *Journal of Geophysical Research*, v. 102, p.4933-4955.
- Bürgmann, R., Fielding, E., and Sukhatme, J., 1998, Slip along the Hayward fault, California, estimated from space-based synthetic aperture radar interferometry: *Geology*, v. 26, p. 559-562.
- Bürgmann, R. Schmidt, D., Nadeau, R., D'Alessio, M., Fielding, E., Lawrence, S., Manaker, D., McEvelly, T., and Murray, M.H., 2000, Earthquake potential along the northern Hayward fault, California, *Science*, 289, 1178-1182.
- Gross, S., and Bürgmann, R., 1998, Rate and state of background stress estimated from the aftershocks of the 1989 Loma Prieta, California, earthquake, *J. Geophys. Res.*, v. 103, p. 4915-4927.
- Johanson, I.A., and Bürgmann, R., 2001, Using point measurements from InSAR to detect transient deformation, *EOS Trans*, AGU, 82 (47), 266, 2001.
- Johanson, I.A., and Bürgmann, R., 2002, An investigation of slow earthquakes on the San Andreas Fault using InSAR, *EOS Trans*, AGU, 83, 2002.
- Manaker, D.M., R. Bürgmann, W.H. Prescott, and J. Langbein, Distribution of interseismic slip rates and the potential for significant earthquakes on the Calaveras fault, central California, *J. Geophys. Res.*, *in press*, 2002.
- Nadeau, R.M., and McEvelly, T.V., 1999, Fault slip rates at depth from recurrence intervals of repeating microearthquakes: *Science*, v. 285, p. 718-721.
- Nadeau, R.M., and T.V. McEvelly, 2000, Spatial and temporal heterogeneity of fault slip from repeating micro-earthquakes along the San Andreas fault in Central California, *Eos Trans. AGU*, v. 81, p. 919.
- Pollitz, F., Bürgmann, R., and Segall, P., 1998, Joint estimation of afterslip rate and postseismic relaxation following the 1989 Loma Prieta earthquake, *J. Geophys. Res.*, v. 103, p. 26,975-26,992.
- Segall, P., R. Bürgmann, and M. Matthews, 2000, Time dependent deformation following the 1989 Loma Prieta earthquake, *J. Geophys. Res.*, 105, 5615-5634.
- Wilber, M.M., and Bürgmann, R., 1999, Slip behavior at depth on the Pajaro segment of the San Andreas fault, California, *EOS Trans. AGU*, 80 (17), 330.

References

- Bryant, W.A., 1985, Faults in the southern Hollister area, San Benito counties, California, *California Division of Mines and Geology Fault Evaluation Report 164*

- Chen, C.W. and H.A. Zebker, Two-dimensional phase unwrapping with use fo statistical models for cost functions in nonlinear optimization, *Journal of the Optical Society of America A*, v. 18, pp. 338-351, 2001.
- Ferretti, A, Prati, C., Rocca, F., 2001, Permanent scatterers in SAR interferometry, *IEEE Transaction on Geoscience and Remote Sensing*, v.39 n.1 pp.8-20
- Gwyther, R.L., C.H. Thurber, M.T. Gladwin, and M. Mee, Seismic and aseismic observations of the 12th August 1998 San Juan Bautista, California M5.3 earthquake, in *3rd San Andreas Fault Conference*, pp. 209-213, Stanford University, 2000.
- Linde, A.T., M.T. Gladwin, M.J.S. Johnston, R.L. Gwyther, and R.G. Bilham, A slow earthquake sequence on the San Andreas fault, *Nature*, 383, 65-68, 1996.

5. Data Availability

Raw and RINEX formatted GPS data files for static surveys of markers in south San Francisco Bay area from 1994-2001. These files typically include greater than six continuous hours of data, recorded at a 30 second collection rate with a 10-degree elevation mask. These data are currently archived at the UNAVCO archive facility in Boulder, and also at the University of California, Berkeley. Photocopies of survey log sheets and site descriptions are also available.

Additional data used in this study included RINEX format files obtained from the U.S. Geological Survey and the Bay Area Regional Deformation Network (BARD). These files include campaign-style surveying (USGS) and continuous GPS stations (BARD) and are available at the NCEDC at UC Berkeley.

For more information regarding data availability, contact:

Dr. Roland Bürgmann
Department of Earth and Planetary Science, University of California, Berkeley
307 McCone Hall
Berkeley, CA 94720-4767
fax(w) (510) 643-9980
e-mail:burgmann@seismo.berkeley.edu
URL:<http://www.seismo.berkeley.edu/~burgmann>
